

Elevated Expression of miR302-367 in Endothelial Cells Inhibits Developmental Angiogenesis via CDC42/CCND1 Mediated Signaling Pathways

Jingjiang Pi^{1,8}, Jie Liu^{1,8}, Tao Zhuang^{1,8}, Lin Zhang¹, Huimin Sun¹, Xiaoli Chen¹, Qian Zhao¹, Yashu Kuang¹, Sheng Peng¹, Xiaohui Zhou¹, Zuoren Yu¹, Ting Tao², Brian Tomlinson³, Paul Chan⁴, Ying Tian⁵, Huimin Fan¹, Zhongmin Liu¹, Xiangjian Zheng⁶, Edward Morrisey⁷, YuZhen Zhang^{1,*}

¹ Key Laboratory of Arrhythmias of the Ministry of Education of China, Research Center for Translational Medicine, Shanghai East Hospital, Tongji University School of Medicine, Shanghai, 200120, China.

² Department of Geriatrics, Ruijin Hospital, Jiaotong University, School of Medicine, Shanghai, 200025, China.

³ Department of Medicine and Therapeutics, The Chinese University of Hong Kong, Hong Kong SAR, China

⁴ Division of Cardiology, Department of Internal Medicine, Wan Fang Hospital, Taipei Medical University, Taipei, Taiwan

⁵ Department of Pharmacology, Center for Translational Medicine, Temple University School of Medicine, Philadelphia, PA 19140, USA.

⁶ Lab of Cardiovascular Signaling, Centenary Institute, Camperdown, NSW 2050, Australia.

⁷ Department of Cell and Developmental Biology (R.W., E.E.M.), Department of Medicine (E.E.M.), Penn Cardiovascular Institute (E.E.M.), and Penn Institute for Regenerative Medicine (E.E.M.), University of Pennsylvania, Philadelphia, Pennsylvania 19104, USA.

⁸These authors contributed equally to this work

*Correspondence

Yuzhen Zhang, MD, PhD

Key Laboratory of Arrhythmias of the Ministry of Education of China

Research Center for Translational Medicine

Shanghai East Hospital, Tongji University School of Medicine,

150 Jimo Rd, Pudong New District, Shanghai, 200120, China

Tel:86-21-61569673, e-mail: yzzhang-tj@tongji.edu.cn

List of Supplementary Materials:

Supplementary Methods

Supplementary Tables

Supplementary Table 1: Partial high throughput RNA sequencing results of lung endothelial cells from miR302-367^{ECTg} mutant comparing to littermate WT control mice.

Supplementary Table 2: Primers for qPCR, Ch-IP and Clone.

Supplementary Table 3: Antibodies for immunostaining, western blot and Co-IP.

Supplementary Figures

Supplementary Figure 1. MiR302-367^{ECTg} mutant mice exhibit elevated expression of miR302-367 in retinal ECs and reduced retinal angiogenesis via inhibition of cell proliferation.

Supplementary Figure 2. MiR302-367^{SMCTg} mutant mice exhibit no significant change of hindbrain developmental angiogenesis *in vivo*.

Supplementary Figure 3. Elevated miR302-367 expression HUVECs reduces the cell motility via observation of cellular actin dynamic changes under live cell station.

Supplementary Figure 4. Endothelial cells from hindbrain of miR302-367^{ECTg} mutant mice display reduced Ccnd1 and Cdc42 expression but not significantly alters the cleaved caspase-3 expression.

Supplementary Figure 5. Constitutive active CDC42 reverses the reduced cell migration and tube formation when miR302-367 expression was elevated in HUVECs under normal and hypoxia condition.

Supplementary Figure 6. MiR302-367 direct target genes CCND1 and CDC42 reverse the miR302-367-mediated reduced cell proliferation.

Supplementary Figure 7. GRB2 promoter sequence analysis.

Supplementary Figure 8. The sequence of mouse and human immature stem-loop and mature miR302a-d and validation of the mechanisms of Target Site Blockers for the pathways miR302 effects on.

Supplementary Figure 9. Target Site Blockers confirm the important role of miR302-Cdc42/Ccnd1 pathway in EC migration and proliferation.

Supplementary video 1: Dynamic cell motility change of HUVECs with elevated miR302-367 expression comparing to the lentiviral-GFP control.

Supplementary Methods

Vascular endothelial cell specific miR302-367 gain-of-function mouse models

Generation of vascular endothelial cell specific miR302-367 gain-of-function mouse R26R-miR302-367^{Tg/+}:Cdh5(PAC)-CreERT2 (miR302-367^{ECTg}) was obtained by crossing a conditional gain-of-function R26R-miR302-367^{Tg/+} mouse line with VE-cadherin (Cdh5) promoter-driven Cre recombinase expression line(1).

Elevated expression of miRNA320-367 in HUVECs via Lentiviral gene transfer

Human umbilical vein endothelial cells (HUVECs, PromoCell) were cultured in endothelial cell growth medium 2 (EGM2, PromoCell). At confluence, cells were harvested by 0.05% trypsin and 0.02% EDTA and subcultured, medium was changed every other day. HUVECs within 8th passage were used, 85–95% confluence for experiments.

Elevated expression of miR302-367 in HUVECs was achieved by lentiviral infection. Lentiviral miR302-367 or control vectors were packaged in human embryonic kidney (HEK) 293T cells (American Type Culture Collection, ATCC, CRL-1573) with X-tremeGENE9 (Roche) of 10 µg miR302-367 or control lentiviral vectors, and package vectors 5 µg psPAX2 and 5 µg pMD2.G (Addgene plasmid 12259). Viral supernatant was collected at 48 hours following transfection, concentrated and applied to HUVECs for infection.

Angiogenesis *in vitro*: fibrin gel bead assay and tube formation assay

Two *in vitro* angiogenesis assays were used to observe the effect of elevated miR320-367 expression in HUVECs. For the fibrin gel bead assay(2), HUVECs with elevated expression of miR320-367 or control lentiviral vector were mixed with Cytodex3 microbeads (Amersham Pharmacia Biotech) at a concentration of 400 HUVECs per bead in EGM-2 (Clonetics) overnight. Cell-coated beads were washed and re-suspended in fibrinogen (Sigma, 2.5 mg/ml), aprotinin (Sigma, 0.15 units/ml) and thrombin (Sigma, 0.625 units/ml) and allowed to clot in 24-well tissue culture plates. A feeder layer of fibroblasts was seeded on top of the fibrin gel and the medium was changed every other day. The number of sprouts, branched sprouts and scattered cells was counted for quantification. In the tube formation assay(3), lentivirus-infected HUVECs were seeded on Matrigel-coated 96-well plates and incubated for 4 hr. Tube formation was quantified by counting the number of branch points and calculating the total tube length in six randomly chosen fields from each well.

Cell migration assay

Boyden chamber and scratch wound healing assay was used to quantify cell migration. In boyden chamber assay, ECs were placed on the upper layer of a cell permeable membrane and culture medium EGM2 containing VEGF (1 ng/µl) below the cell permeable membrane of the transwell (Falcon 353097). Following 4 hours incubation, the cells that have migrated through the membrane were stained by crystal violet staining solution and counted. In scratch wound healing assay, equal numbers of ECs were plated in 6-well tissue culture plate to achieve 90% confluence. A vertical wound was created by a 0.1 µl pipette tip. The cells were cultured with FBS-reduced DMEM medium (0.1%–0.5% FBS) and images of the wound were captured at designated times to assess wound closure rate.

Cell proliferation assay

Cell count, MTT assay (3-(4, 5-Dimethylthiazol-2-yl)-2, 5-diphenyltetrazolium bromide), Cell Cycle (PI staining) and Ki67 immunostaining were used to quantify cell proliferation.

In Cell Count, HUVECs were seeded at an initial density of 7.5×10^4 per well in a 12-well plate which were counted at designated time-points for cell counting assay.

In MTT assay, HUVECs were seeded in a flat-bottom 96-well cell culture plate at an initial density of 5×10^3 cells per well and allowed to grow for 48 hours, $10 \mu\text{l}$ of MTT (5 mg/ml) solution (Sigma) was added to each well followed by 4-hour incubation at 37°C , the media removed and $80 \mu\text{l}$ mixture of 40 ml isopropanol plus $44 \mu\text{l}$ 37% HCl added to each well, then vibrated on a shaking table for 10 minutes to dissolve the formed formazan. The plate was scanned with a microplate reader (Bio-Rad) at 570 nm for measuring the absorbance.

For propidium Iodide (PI) cell cycle analysis, HUVECs were starved in DMEM supplemented with 5% charcoal-stripped serum or 0.5% regular FBS. After 24 hours, medium was changed to DMEM with 10% normal FBS. Cells were harvested at designated time points, processed by standard methods by staining cell DNA with propidium iodide (PI), 10,000 cells per sample were analyzed by a flow cytometer (BD Biosciences, Mansfield, MA, USA).

For Ki67 immunofluorescence staining analysis, HUVECs were fixed in 4% neutral-buffered para-formaldehyde non-specific binding sites were blocked with PBS containing 10% normal goat serum. The HUVECs were further incubated with the primary antibodies against Ki-67 followed by an Alexa 488-conjugated secondary antibody (Thermo Fisher Scientific, Danvers, Massachusetts, USA). The HUVECs were mounted using Prolong Gold anti-fade mountant with DAPI (Thermo Fisher Scientific).

Dynamic cell motility measurement under live cell station

The viable HUVECs were planted at density of 1.5×10^5 in 6-well plate and cultured for 12 hours, then transfected with Life-act GFP plasmid. The cells were placed under live cell station microscopy and photographs taken every two minutes to measure the dynamic change of cell mobility(4). Filopodia, lamellipodia, cortex and stress fiber quantification methods were described previously(5-7).

Quantitation of G-actin, F-actin and GTPase activity assay

The amount of globular G-actin and filamentous F-actin was determined using the G-actin/F-actin *in vivo* assay kit from Cytoskeleton (Denver, CO, USA), and the Cdc42 GTPase activity was measured using the G-LISA activation assay biochem kits from Cytoskeleton Inc. (Denver, CO), following the manufacturer's instruction.

RNA purification, RT-qPCR and miRNA quantitation

Total RNA was isolated by Trizol from ECs of newborn mouse lung or HUVECs, reverse transcribed by SuperScript First Strand Synthesis System (Invitrogen, Carlsbad, CA, USA). Expression of genes was quantified by real time PCR analysis (RT-qPCR) with the primers listed in supplement table 1 (Table S1) of the supplementary material. For miRNA quantification, total RNA was extracted from isolated ECs of lung microvessels or HUVECs using a miRNeasy mini kit and the relative microRNA levels were measured by the TaqMan miRNA reverse transcription kit and miRNA assay kit following the manufacturer's instruction.

RNA high-throughput sequence of vascular endothelial cells isolated from mouse lung

Total RNA of the green ECs FACS sorting ECs from lung of R26R-tdTomato-EGFP mouse line (JaxMice, stock number 007576) mated with miR302-367 gain-of-function or control mouse for high-throughput sequencing. RNA samples extracted with Trizol were subjected to 100 bp x 2 non-strand-specific paired-end RNA-sequence analyses by Genome Center of WuXi App Tec(8).

Western blot analysis

Total protein extracts (20-50 μg) from HUVECs were resolved on SDS-PAGE gels and transferred to

PVDF membranes for western blotting. Antibodies used in this article were listed in the supplementary table S3.

Co-immunoprecipitation (Co-IP)

For GRB2/PAK1 and CCND1/CDK4 immunoprecipitation, one 145 mm dish of cells was harvested by trypsinization, washed with PBS twice, and lysed with RIPA buffer containing 1 x PIC by rotating for 1 hour at 4°C. Cell debris was removed by centrifugation, cell lysate was split into two parts (5% of lysate was saved as input), and 8 µg anti-GRB2/PAK1/CCND1/CDK4 antibodies and 8µg IgG was used for immunoprecipitation at 4°C overnight. 30 µl protein G beads were used for pull-down at 4°C for 1 hour. Beads were washed with RIPA buffer three times, and bead-bound proteins were lysed with cell lysis buffer (50 mM Tris-Cl, pH 6.8, containing 2% SDS). Lysates and saved inputs were used for western blot detection of PAK1/GRB2/CCND1/CDK4.

CDC42-GTP Pull-Down assay

Briefly, cells were lysed in RIPA buffer and centrifuged at 15,000 rpm for 10 min at 4 °C. Supernatants were mixed with PAK-GST beads which binds specifically to GTP-bound, and not GDP-bound, CDC42 proteins (Cytoskeleton). Levels of CDC42-GTP was detected by western immunoblotting using anti-CDC42 antibodies.

Chromatin Immunoprecipitation (ChIP)

3×10⁷ HUVECs were harvested for ChIP experiment. Cells were cross-linked with 1% formaldehyde at room temperature for 10 min, and then neutralized with 125 mM glycine for 5 min. Cells were rinsed with ice-cold PBS twice and scraped into 1 ml of ice-cold PBS. Cells were re-suspended in 0.3 ml of lysis buffer and sonicated. After centrifugation, supernatants were collected and diluted in IP dilution buffer followed by immunoclearing with protein A-sepharose for 2 hours at 4°C. 5 µg anti-KLF2 (Cat No: ab203591, Abcam); or control IgG (Cat No: 2729S, CST) were used for immunoprecipitation. After immunoprecipitation, 45 µl protein A-Sepharose was added and incubated for another hour. Precipitates were washed, and DNA was purified after de-crosslinking for real-time PCR. Primers used are listed in Supplementary Tables 2.

3'-UTR Luciferase Reporter Assay

The 3'-UTR of *CCND1* or *CDC42* mRNA containing miR302-367 binding sequence was inserted into pMIR-REPORT, a microRNA 3'-UTR Luciferase vector. Mutagenesis of the seed sequences from the miR302-367 binding sites of *CCND1* or *CDC42* was generated by PCR-mediated site-directed mutagenesis. The final sequence was validated by DNA sequencing. Luciferase activity was determined 48 hours after transfection using Dual-Luciferase assay kits (Promega, Madison, WI, USA). Individual luciferase activity was normalized to the corresponding Renilla-luciferase activity(9).

Plasmid construct of *GRB2* promoter luciferase reporter.

pGRB2(1027) is the human *GRB2* promoter-luciferase reporter construct which spans positions -820 to +207 relative to the transcription start site and was amplified with PCR using genomic DNA isolated from HUVECs as a template. Then, the digested PCR product was cloned into the HindIII-XhoI sites of pGL3-basic reporter vector (Promega). The details of the primers are shown in Supplementary Table S2.

Promoter luciferase reporter assay

The promoter of *GRB2* gene containing two KLF2 binding motifs was inserted into a pGL3 promoter Luciferase vector. The final sequence was validated by DNA sequencing. Luciferase activity was determined

48 hours after transfection using Dual-Luciferase assay kits (Promega). Individual luciferase activity was normalized to the corresponding Renilla-Luciferase activity.

Target site blockers for validation of the pathway contributing to endothelial cell migration and proliferation when elevated miR302 expression.

MicroRNAs usually regulate gene expression of multiple targets. Identification of these targets is important to understanding the function of the microRNA. Target site blockers (TSB) are used to determine which pathway contributes significantly to the phenotype observed upon microRNA expression. The custom-designed TSBs with phosphorothioate backbone modifications from Exiqon (miRCURY LNATM microRNA TSB) were used *in vivo* and *in vitro* to selectively silence the activity of miR-302 cluster on mouse and human *Ccnd1/CCND1* and *Cdc42/CDC42*, respectively, and the retinal *in vivo* developmental sprout angiogenesis and cell proliferation, as well as cell migration and proliferation in culture HUVECs were observed to validate the importance of these miR302 target genes in EC migration and proliferation. TSB sequences are designed with a large arm that covers the miRNA binding site and a short arm outside the miRNA seed to ensure target specificity of 3'UTR of *Ccnd1/CCND1* or *Cdc42/CDC42*(10).

Intraocular injection was performed to observe the *in vivo* effects of TSB as previous described(11). In brief, Buprenorphine (0.1 mg/kg) was injected in pups subcutaneously one hour prior to the procedure. The pups were anesthetized by hypothermia and the skin over the eyelid was cleaned with Betadine followed by water and 70% ethanol. Intraocular injections were performed under a dissecting microscope with a 30_{1/2}-gauge needle attached to a 5 µl glass syringe (Hamilton, Reno, USA), the needle was positioned 1 mm posterior to the limbus and 3 µl (Target site blockers, 0.4 mg/20 g) was slowly (3-5 seconds) injected into the vitreous chamber of the eye. While in culture HUVECs, the concentration of the TSBs was 50 nM.

siRNA transfections

Cells were plated 24 hours before transfection at 50% confluence. KLF2 siRNA and control siRNA transfections were performed with LipofectamineRNAiMAX (Invitrogen). The following siRNA oligonucleotides from Sigma were used: KLF2 siRNA1: SASI_Hs01_00227239; KLF2 siRNA2: SASI_Hs02_00349172, KLF2 siRNA3 SASI_Hs02_00349173. Control siRNA was purchased from Sigma. For single KLF2 siRNA transfection, each individual siRNA was used at 60 nM concentration

Hypoxia experiment

For hypoxia treatment, HUVECs were maintained in glucose-free DMEM at 37 °C in an atmosphere of 5% CO₂, 1% O₂, and 94% N₂. Transwell, tube formation and wound healing experiments were operated under this hypoxia condition.

References

1. Wang Y, Nakayama M, Pitulescu ME, Schmidt TS, Bochenek ML, Sakakibara A, et al. Ephrin-B2 controls VEGF-induced angiogenesis and lymphangiogenesis. *Nature*. 2010; 465: 483-6.
2. Nehls V, Drenckhahn D. A novel, microcarrier-based in vitro assay for rapid and reliable quantification of three-dimensional cell migration and angiogenesis. *Microvasc Res*. 1995; 50: 311-22.
3. Arnaoutova I, Kleinman HK. In vitro angiogenesis: endothelial cell tube formation on gelled basement membrane extract. *Nat Protoc*. 2010; 5: 628-35.
4. Zhao Y, Mao Q, Liu Y, Zhang Y, Zhang T, Jiang Z. Investigation of cytotoxicity of phosphoryl choline modified single-walled carbon nanotubes under a live cell station. *Biomed Res Int*. 2014; 2014: 537091.
5. Barry DJ, Durkin CH, Abella JV, Way M. Open source software for quantification of cell migration, protrusions, and fluorescence intensities. *J Cell Biol*. 2015; 209: 163-80.
6. Ryan GL, Petroccia HM, Watanabe N, Vavylonis D. Excitable actin dynamics in lamellipodial protrusion and retraction. *Biophys J*. 2012; 102: 1493-502.
7. Deibler M, Spatz JP, Kemkemer R. Actin fusion proteins alter the dynamics of mechanically induced cytoskeleton rearrangement. *PLoS One*. 2011; 6: e22941.
8. Guo R, Zheng L, Park JW, Lv R, Chen H, Jiao F, et al. BS69/ZMYND11 reads and connects histone H3.3 lysine 36 trimethylation-decorated chromatin to regulated pre-mRNA processing. *Mol Cell*. 2014; 56: 298-310.
9. Anokye-Danso F, Trivedi CM, Jühr D, Gupta M, Cui Z, Tian Y, et al. Highly efficient miRNA-mediated reprogramming of mouse and human somatic cells to pluripotency. *Cell Stem Cell*. 2011; 8: 376-88.
10. Messina A, Langlet F, Chachlaki K, Roa J, Rasika S, Jouy N, et al. A microRNA switch regulates the rise in hypothalamic GnRH production before puberty. *Nat Neurosci*. 2016; 19: 835-44.
11. Pi J, Tao T, Zhuang T, Sun H, Chen X, Liu J, et al. A MicroRNA302-367-Erk1/2-Klf2-S1pr1 Pathway Prevents Tumor Growth via Restricting Angiogenesis and Improving Vascular Stability. *Circ Res*. 2017; 120: 85-98.

Supplement Table 1: Partial high throughput RNA sequencing results of lung endothelial cells from miR302-367^{ECTg} mutant comparing to littermate WT control mice

Symbol	GeneID	FPKM(4c)	FPKM(3m)	Log2.fold_change
CCND1	12443	7.69436	6.22739	-0.305175
CDC42	12540	380.511	189.806	-1.00341
GRB2	14784	72.6484	35.8417	-1.01929
KLF2	16598	121.611	235.352	0.952549
MAPK3	26417	172.712	117.893	-0.550896
MAPK1	26413	59.3909	41.3669	-0.521765

Supplemental table 2: Primers for qPCR, Chip and Clone

qPCR Primers (Human)

Name	Forward	Reverse
<i>CCND1</i>	5-TCCT CTCCAGAGTGATCAAGTG-3	5-TTGGGG TCCATGTTCTGC-3
<i>CDK4</i>	5-ATGGCTACCTCTCGATATGAGC-3	5-CATTGGGGACTCTCACACTCT-3
<i>CDK6</i>	5-GCTGACCAGCAGTACGAATG-3	5-GCACACATCAAACAACCTGACC-3
<i>CDKN1A</i>	5-TGTCCGTCAGAACCCATGC-3	5-AAAGTCGAAGTTCATCGCTC-3
<i>CDKN1B</i>	5-AACGTGCGAGTGTCTAACGG-3	5-CCCTCTAGGGGTTTGTGATTCT-3
<i>CDC42</i>	5-CCCGGTGGAGAAGCTGAG-3	5-CGCCCACAACAACACACTTA-3
<i>RAC1</i>	5-GTAAACCTGCCTGCTCATC-3	5-GCTTCATCAAACACTGTCTTG-3
<i>GAPDH</i>	5-ATGGAATCCCATCACCATCTT-3	5-CGCCCCACTTGATTTTGG-3
<i>ACTIN</i>	5-CATGTACGTTGCTATCCAGGC-3	5-CTCCTTAATGTCACGCACGAT
<i>KLF2</i>	5-TTCGGTCTCTTCGACGACG-3	5-TGCGAACTCTTGGTGTAGGTC-3
<i>GRB2</i>	5-CTGGGTGGTGAAGTTCAATTCT-3	5-GTTCTATGTCCCGCAGGAATATC-3

qPCR Primers (Mouse)

Name	Forward	Reverse
<i>Ccnd1</i>	5-GCGTACCCTGACACCAATCTC-3	5-ACTTGAAGTAAGATACGGAGGGC-3
<i>Cdc42</i>	5-CCCATCGGAATATGTACCAACTG-3	5-CCAAGAGTGTATGGCTCTCCAC-3
<i>Mapk1</i>	5-GGTTGTTCCCAAATGCTGACT-3	5-CAACTTCAATCCTCTTGTGAGGG-3
<i>Mapk3</i>	5-TCCGCCATGAGAATGTTATAGGC-3	5-GGTGGTGTGATAAGCAGATTGG-3

ChIP

Name	Forward	Reverse
<i>GRB2 Promoter ChIP</i>	5-TCCCTCCGACTCCAGATA-3	5-CAGGTGTAGAATGCCAGATT-3
<i>GAPDH ChIP</i>	5-GCTTGCCCTGTCCAGTTAAT-3	5-TAGCTCAGCTGCACCCTTTA-3

GRB2 promoter clone primer (-820 to +207)

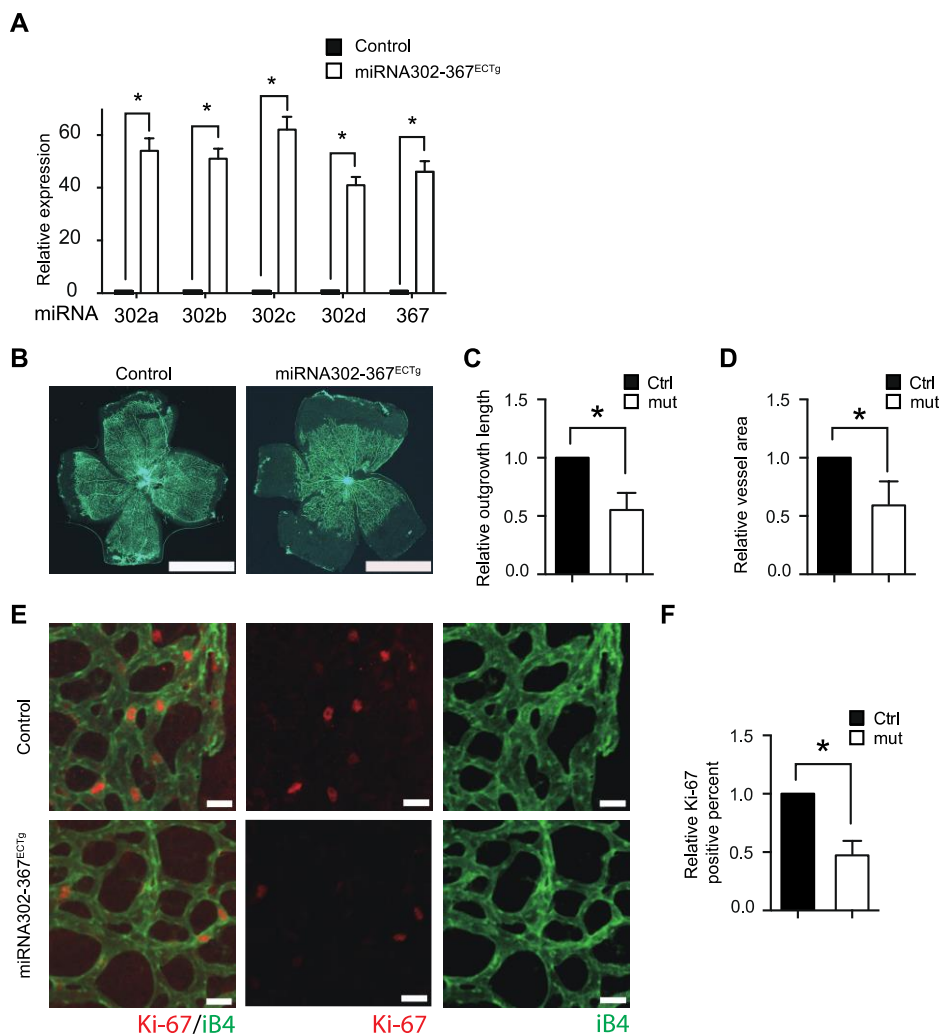
Name	Forward	Reverse
<i>GRB2 Promoter</i>	5-AGGAAGTCATGGGAACGCAG-3	5-CTTGGCTCTGGGGATTTTGC-3

Supplemental table 3: Antibodies for immunostaining, western blot and Co-IP

Name	Company	Blocking buffer	Category	Dilute conc.	Dilution solution
iB4	Vector	2% BSA+0.1% Triton	B-1205	1:25	2% BSA+0.1% Triton
Ki-67	Abcam	Whole-mount: 2% BSA +0.1% Triton	ab15580	1:25	2% BSA+0.1% Triton
	Abcam	In vitro: 5% BSA +0.1% Triton	ab15580	1:500	5% BSA+0.1% Triton
CYCLIN (CCND1)	Cell signalling	5% nonfat dry milk	2922	1:1000	1% nonfat dry milk
P21	Cell signalling	5% nonfat dry milk	2946	1:1000	1% nonfat dry milk
P27	Cell signalling	5% nonfat dry milk	2552	1:1000	1% nonfat dry milk
CDK4	Abcam	5% nonfat dry milk	ab199728	1:2000	1% nonfat dry milk
CDK6	Cell signalling	5% nonfat dry milk	3136	1:1000	1% nonfat dry milk
RB	Cell signalling	5% nonfat dry milk	9309	1:2000	1% nonfat dry milk
p-RB(S807/811)	Cell signalling	5% nonfat dry milk	8516	1:1000	1% nonfat dry milk
E2F1	Cell signalling	5% nonfat dry milk	3742	1:1000	1% nonfat dry milk
RAC1	Thermo Fisher	5% nonfat dry milk	16118	1:1000	3% BSA and 0.1% Triton
CDC42	Thermo Fisher	5% nonfat dry milk	16119	1:1000	3% BSA and 0.1% Triton
GAPDH	Abcam	5% nonfat dry milk	ab8245	1:10000	1% nonfat dry milk
ACTIN	Cell signalling	5% nonfat dry milk	4967	1:10000	1% nonfat dry milk
p-N-WASP (Y256)	Abcam	5% nonfat dry milk	ab23395	1:500	1% nonfat dry milk
N-WASP	Abcam	5% nonfat dry milk	ab126626	1:2500	1% nonfat dry milk
p-WASP (Y290)	Abcam	5% nonfat dry milk	ab59278	1:1000	1% nonfat dry milk
WASP	Abcam	5% nonfat dry milk	ab68182	1:1000	1% nonfat dry milk
p-WAVE(Y125)	Abcam	5% nonfat dry milk	ab59280	1:1000	1% nonfat dry milk
WAVE	Abcam	5% nonfat dry milk	ab50356	1:500	1% nonfat dry milk
RAS	Cell signalling	5% nonfat dry milk	3965	1:2000	1% nonfat dry milk
RHOA	Abcam	5% nonfat dry milk	ab54835	1:1000	1% nonfat dry milk
KLF2	Abcam	5% nonfat dry milk	ab203591	1:500	1% nonfat dry milk
GRB2	Abcam	5% nonfat dry milk	ab32037	1:2000	1% nonfat dry milk
PAK1	Abcam	5% nonfat dry milk	ab183894	1:1000	1% nonfat dry milk
p-PAK1(T212)	Abcam	5% nonfat dry milk	ab75599	1:500	1% nonfat dry milk
p-PAK2(S192)	Abcam	5% nonfat dry milk	ab79505	1:1000	1% nonfat dry milk
p-PAK4(S560)	Abcam	5% nonfat dry milk	ab134097	1:1000	1% nonfat dry milk
COFILIN	Abcam	2.5% BSA	ab42824	1:1000	1% nonfat dry milk
p-COFILIN(S3)	Abcam	2.5% BSA	ab131274	1:500	1% nonfat dry milk
LIMK	Abcam	5% nonfat dry milk	ab95186	1:1000	1% nonfat dry milk
p- LIMK(T508)	Abcam	5% nonfat dry milk	ab194798	1:500	1% nonfat dry milk

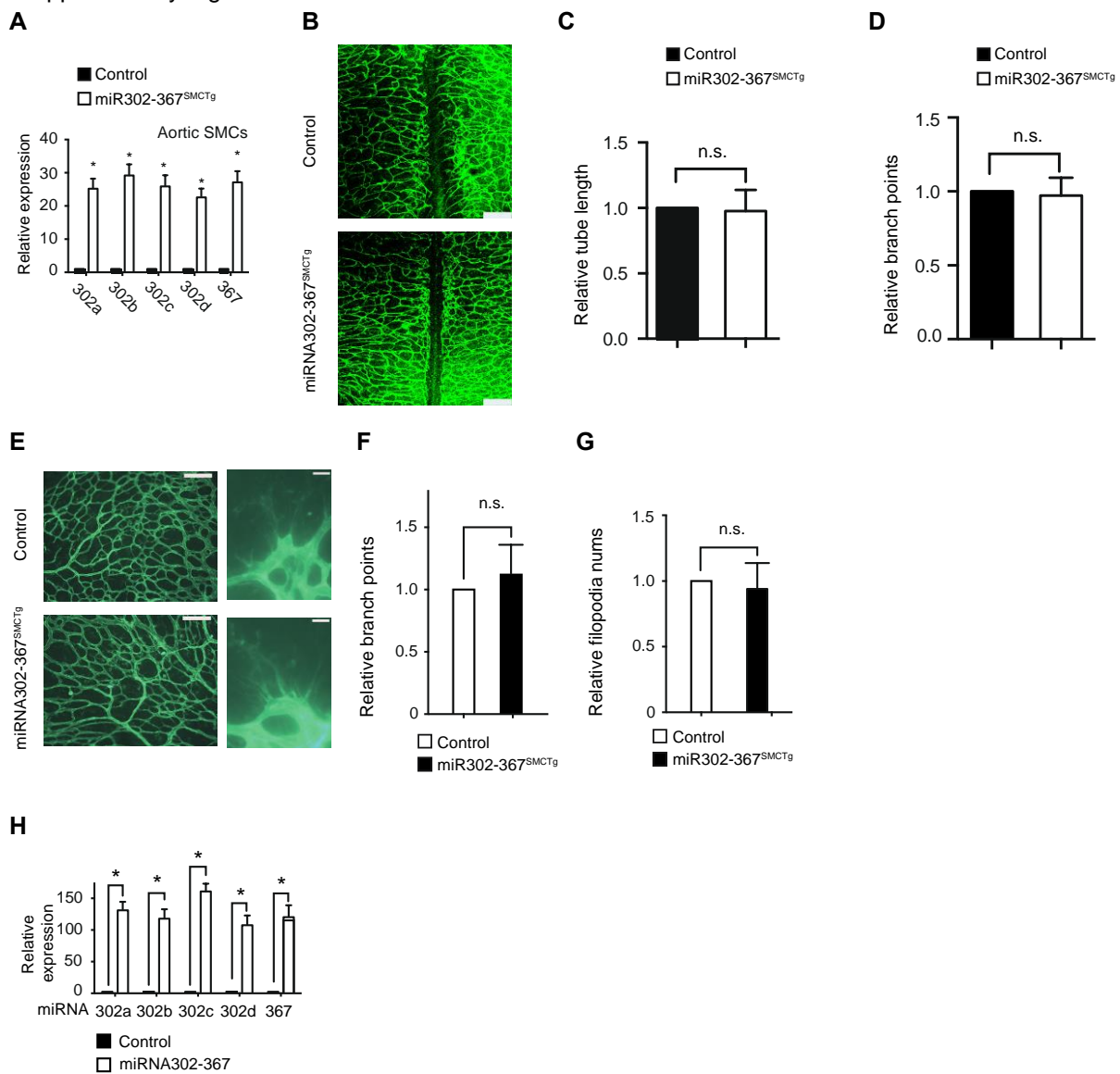
Supplementary Figures:

Supplementary Figure 1



Supplementary Figure 1. MiR302-367^{ECTg} mutant mice exhibit elevated expression of miR302-367 in retinal ECs and reduced retinal angiogenesis via inhibition of cell proliferation. (A) Elevated expression of miR302-367 cluster in retinal ECs of miR302-367^{ECTg} mutant comparing to WT littermate control mice. (B-D) MiR302-367^{ECTg} mutant mice exhibit a significant reduction of retinal angiogenesis quantified by outgrowth length (B, C) and vessel area (B, D). (E-F) MiR302-367^{ECTg} mutant mice exhibit reduced Ki67 staining in retina with quantification. Data quantification is mean \pm S.E.M (n = 6). All data were analyzed using Student's t-test unless otherwise noted. *, P<0.05; **, P<0.01. Scale bars: B, 2 mm; E, 50 μ m.

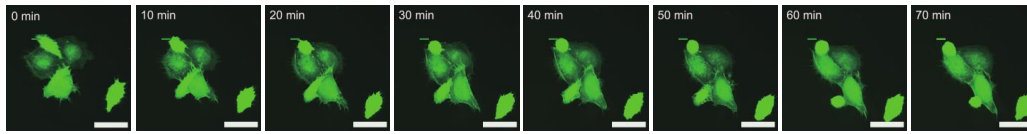
Supplementary Figure 2



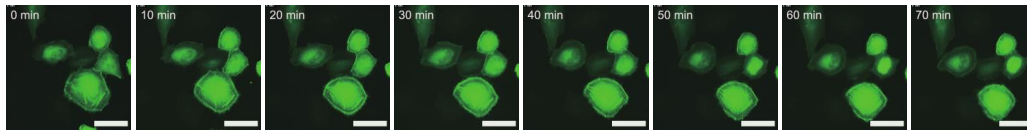
Supplementary Figure 2. MiR302-367^{SMCTg} mutant mice exhibit no significant change of hindbrain developmental angiogenesis *in vivo*. (A) Elevated expression of miR302-367 in aortic smooth muscle cells of miR302-367^{SMCTg} mutant comparing to WT littermate control mice. (B-D) MiR302-367^{SMCTg} mutant mice exhibit no significant change of embryonic hindbrain angiogenesis as quantification by the reduction of relative tube length (B, C) and branch points (B, D) at ventricular side of the hindbrain. (E-G) MiR302-367^{SMCTg} mutant mice exhibit no significant change of retinal angiogenesis at P6 as shown by the reduction of retinal relative branch points (E, F) and filopodia numbers (E, G). (H) All members of miR302-367 are significantly increased in HUVECs when infection of lentiviral-miR302-367 compared to control lentiviral-GFP. Data quantification is mean \pm S.E.M. (n = 3). All data were analyzed using Student's t-test unless otherwise noted. n.s., not significance; *, P<0.05. Scale bars: B, 250 μ m; E, 100 μ m (left), 50 μ m (right).

Supplementary Figure 3

A Control



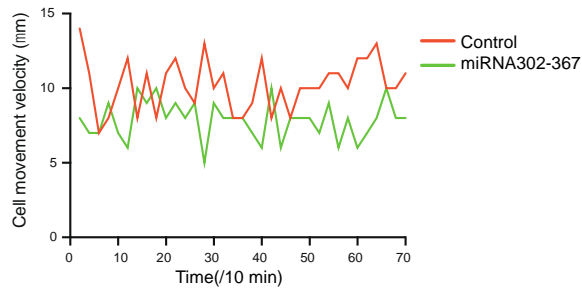
B miRNA302-367



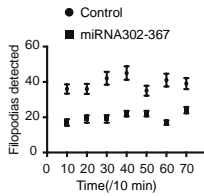
C



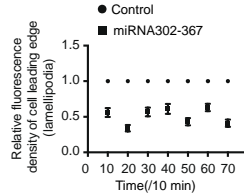
D



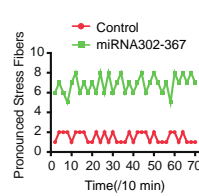
E



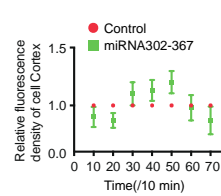
F



G

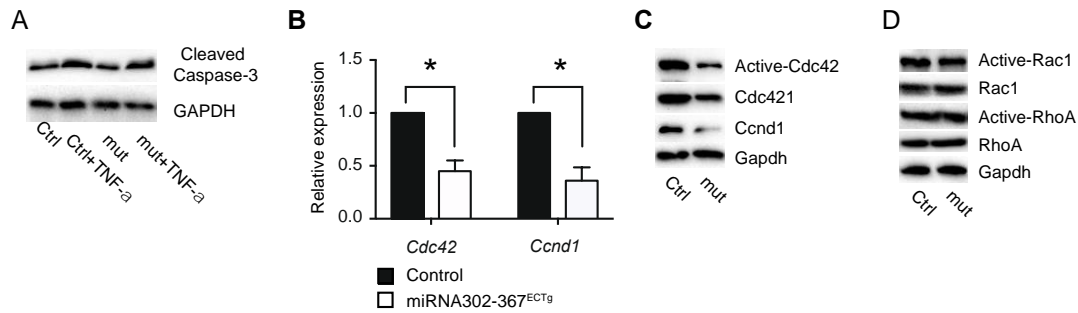


H



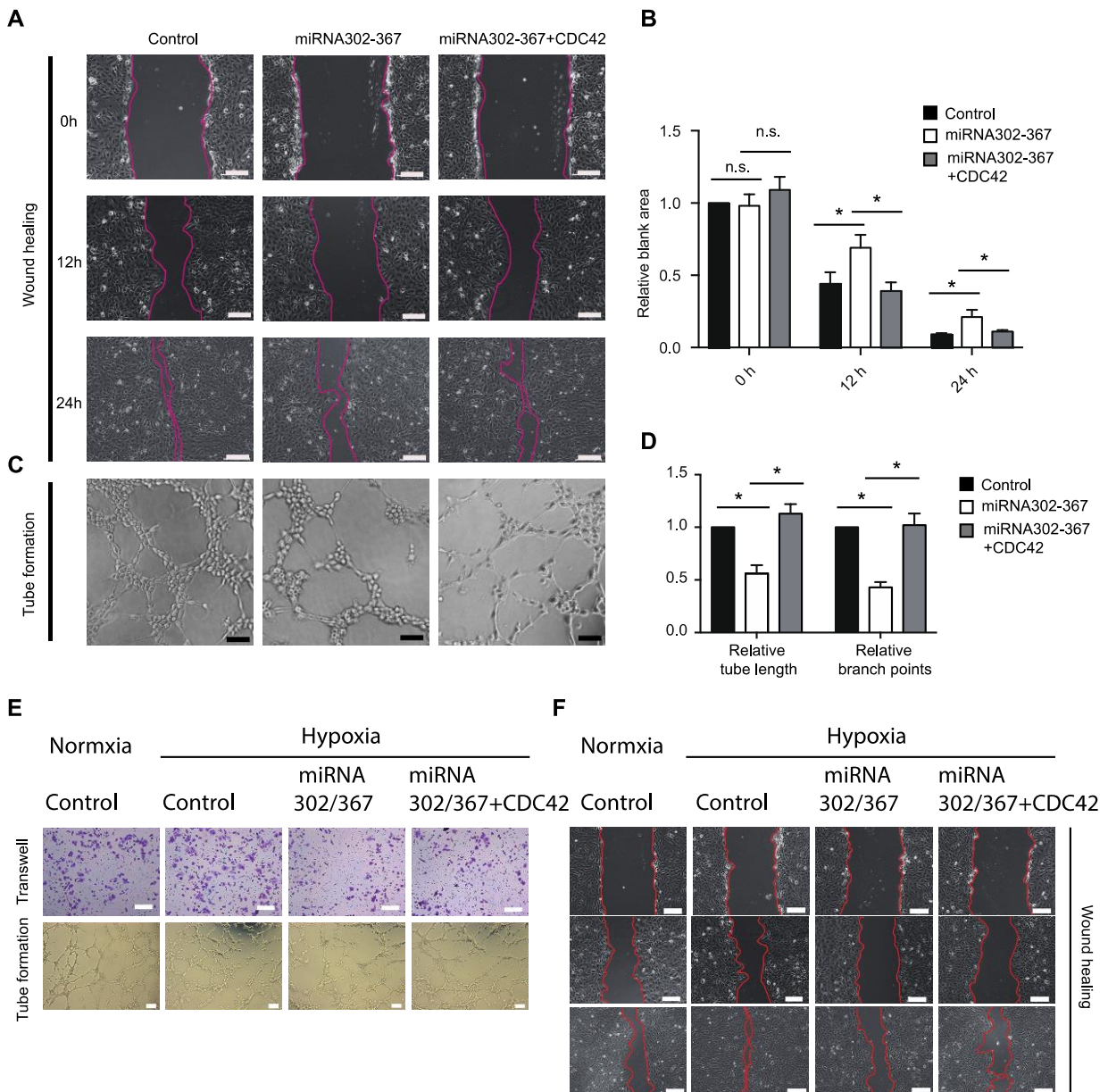
Supplementary Figure 3. Elevated miR302-367 expression in HUVECs reduces the cell motility via observation of cellular actin dynamic changes under live cell station. (A-B) The representative images of dynamic change of cell motility under live cell station in HUVECs transfected with Life-act GFP control plasmid (A) and HUVECs with elevated miR302-367 expression (B). (C) The cell center movement trajectory of HUVECs with Life-act GFP control or elevated miR302-367 expression. (D) The cell movement velocity of HUVECs with Life-act GFP control or elevated miR302-367 expression. (E-H) The detected filopodias (E), density of cell leading edge lamellipodias (F), detected pronounced stress fibers (G) and density of cell cortex actin (H) of HUVECs with Life-act GFP control or elevated miR302-367 expression. Data quantification is mean \pm S.E.M. (n = 3). All data are analyzed using student's t-test unless otherwise noted. *, P<0.05. Scale bars: A. 100 μ m.

Supplementary Figure 4



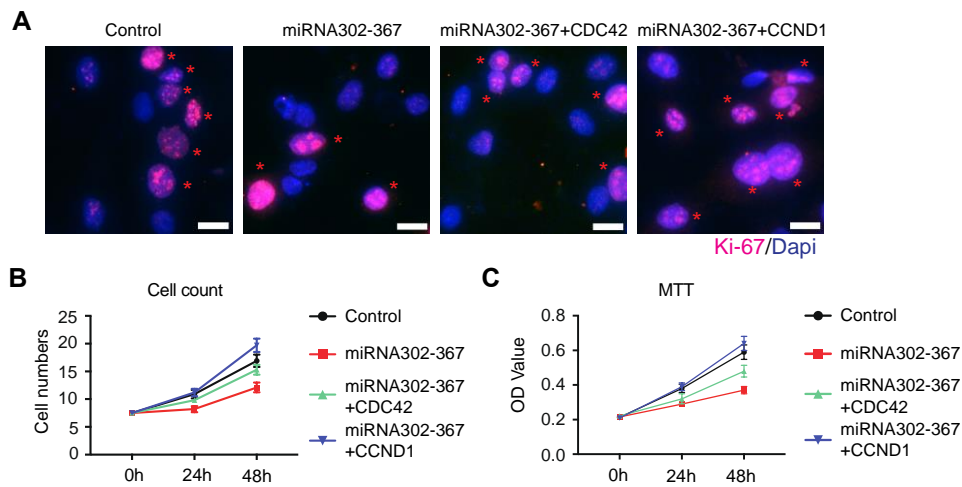
Supplementary Figure 4. Endothelial cells from hindbrain of miR302-367^{ECTg} mutant mice display reduced Ccnd1 and Cdc42 expression but not significantly alter the cleaved caspase-3 expression (A) ECs of hindbrain from miR302-367^{ECTg} mutant mice exhibit no significant change of cleaved caspase-3 expression at basal and TNF α treated condition when compared with the WT littermate control mice. **(B-C)** ECs of hindbrain from miR302-367^{ECTg} mutant mice exhibit reduced Ccnd1 and Cdc42 in RNA and protein level by qPCR and western blot analysis. **(D)** ECs of hindbrain display no difference on RhoA and Rac1 protein expression between miR302-367^{ECTg} mutant and littermate WT control mice. Data quantification is mean \pm S.E.M. (n = 3). All data are analyzed using student's t-test unless otherwise noted. *, P<0.05.

Supplementary Figure 5



Supplementary Figure 5. Constitutive active CDC42 reverses the reduced endothelial cell migration and tube formation caused by elevated miR302-367 expression in normal and hypoxia condition (A-B) Constitutive active CDC42 reverses the reduced cell migration in HUVECs when elevated miR302-367 expression by scratch wound healing assay, the representative images (A) and quantification (B). (C-D) Constitutive active CDC42 reverses the tube formation in HUVECs when elevated miR302-367 expression, the representative images (C) and quantification (D). (E-F) Constitutive active CDC42 reverses the cell migration in HUVECs when elevated miR302-367 expression under hypoxia condition by Boyden chamber assay (E, top) and tube formation (E, bottom) and scratch wound healing assay (F). Data quantification is mean \pm S.E.M. (n = 3). All data were analyzed using Student's t-test unless otherwise noted. *, P<0.05. Scale bars: A, 200 μ m; C, 100 μ m; E, 100 μ m (top), 100 μ m (bottom); F, 200 μ m.

Supplementary Figure 6



Supplementary Figure 6. MiR302-367 direct target genes CCND1 and CDC42 reverse the miR302-367-mediated reduced cell proliferation. (A-C) CCND1 and CDC42 reverse the reduced cell proliferation when miR302-367 expression was elevated in HUCECs as measured by Ki67 immunostaining (A), cell count (B) and MTT assay (C). Data quantification is mean \pm S.E.M. (n = 3). All data were analyzed using Student's t-test unless otherwise noted. *, P<0.05. Scale bars: A, 100 μ m.

Supplementary Figure 7

A

GRB2 promoter sequence

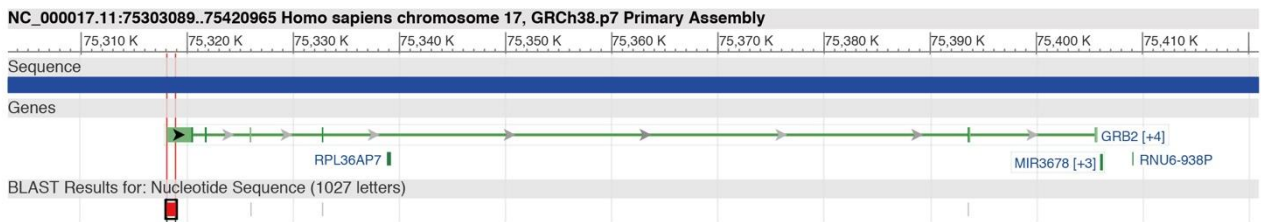
ATCTGGCTTACAGGGGGTTCGGAAGCCTGTCCTCACCGTCTCGGGGGTTGTGGCCCCGCCCCCTCCCTATATGCACCCC
 TGGAAACCAGCAAGTCCCAGACAAGGAGAGCGGAGGAGGAAGTCATGGGAACGCAGCCTCCAGTTGTAGCAGGTTTCA
 CTATTCCTATGCTGGGTACACAGTGAGAGTACTCACTTTTCACTTGCTTGGCTTTAGATTGGCCATGGCTTTCATCCT
 GTGTCCCCTGACCTGTCCAGGTGAGTGTGAGGGCAGCACTGGGAAGCTGGAGTGCTGCTTGTGCCTCCCTCCCAGTG
 GGCTGTGTTGACTGCTGCTCCCACCCCCTACCGATGGTCCCAGGAAGCAGGGAGAGTTGGGGAAGGCAAGATTGGAA
 AGACAGGAAGACCAAGGCCTCGGCAGAACTCTGTCTTCTCCTCACTTCTGGTCCCCTGTGGTGATGTGCCTGTAATC
 TTTTTCTCACCCAAACCCCTTCCCACGACAAAAACAAGACTGCCTCCCTCTTCCGGGAGCTGGTGACAGCCTTGG
 GCCTTTCAGTCCCAAAGCGGCCGATGGGAGTCTCCCTCCGACTCCAGATATGAACAGGGCCCAGGCCTGGAGCGTTTG
 CTGTGCCAGGAGGGCGGCAGCTCTTCTGGGCAGAGCCTGTCCCCGCCTTCCCTCACTCTTCCCTCATCCTGCTTCTCTTT
 CCTCGCAGATGATAAAAGGAATCTGGCATTCTACACCTGGACCATTGATTGTTTTATTTTGAATTGGTGTATATCATGA
 AGCCTTGCTGAACTAAGTTTTGTGTATATATTAAAAAATAAATCAGTGTTTAAATAAAGACCATGTACTTAATCCTT
 TAACTCTGCGGATAGCATTGGTAGGTAGTGATTAACGTGAATAATAAATACACAATGAATTTTCAGTGACCGCCCAG
 CTCTCCACATCCCCTGGGTGATGGGCCACCGGGGCAAGAGGGGAAGGAGTATGGAAGCCATCGCCAAATATGACTTC
 AAAGTACTGCAGACGACGAGCTGAGCTTCAAAGGGGGGACATCCTCAAGGTTTTGAACGAAGAATGTGATCAGAA
 CTGGTACAAGGCAGAGCTTAATGGAAAAGACGGCTTCAATCCCAAGAACTACATAGAAATGAAACCACATCCGTGGTT
 TTTTGGCAAAATCCCCAGAGCCAAGGCAGAAGAAATGCTTAGCAAACAGCGGCACGATGGGGCCTTCTTATCCGAG
 AGAGTGAGAGCGCTCCTGGGGACTTCTCCCTCTCTGTCAAGTTTGGAAACGATGTGCAGCACTTCAAGGTGCTCCGA
 GATGGAGCCGGGAAGTACTTCTCTGGGTGGTGAAGTTCAATTCTTTGAATGAGCTGGTGGATTATCACAGATCTACAT
 CTGTCTCCAGAAACCAGCAGATATTCTGCGGGACATAGAACAGGTGCCACAGCAGCCGACATACGTCCAGGCCCTCT
 TTGACTTTGATCCCCAGGAGGATGGAGAGCTGGGCTTCCGCCGGGAGATTTTATCCATGT-
 CATGGATAACTCAGACCCCACTGGTGGAAAGGAGCTTGCCACGGGCAGACCGGCATGTTTCCCGCAATTATGCACCCCGTGAACC
 GGAAAGCTCTAA

B

GRB2 promoter cloned sequence -820 to +207

GAAGTCATGGGAACGCAGCCTCCAGTTGTAGCAGGTTTCACTATTCCTATGCTGGGGTACACAGTGAGAGTACTCACTTTTCACTTGCT
 TGCTCTTAGATTGGCCATGGCTTTCATCCTGTGTCCCCTGACCTGTCCAGGTGAGTGTGAGGGCAGCACTGGGAAGCTGGAGTGCTG
 CTGTGCCTCCCTTCCAGTGGGCTGTGTTGACTGCTGCTCCCACCCCCTACCGATGGTCCCAGGAAGCAGGGAGAGTTGGGGAAGG
 CAAGATTGGAAAGACAGGAAGACCAAGGCCTCGGCAGAACTCTGTCTTCTCCTCACTTCTGGTCCCCTGTGGTGATGTGCCTGTAAT
 CTTTTTCTCACCCAAACCCCTTCCCACGACAAAAACAAGACTGCCTCCCTCTTCCGGGAGCTGGTGACAGCCTTGGCCTTTCAGT
 CCCAAAGCGGCCGATGGGAGTCTCCCTCCGACTCCAGATATGAACAGGGCCCAGGCCTGGAGCGTTTGTGTGCCAGGAGGGCGGCAG
 CTCTTCTGGGCAGAGCCTGTCCCCGCCTTCCCTCACTCTTCTCATCCTGCTTCTTTTTCTCGCAGATGATAAAAGGAATCTGGCATT
 CTACACCTGGACCATTGATTGTTTTATTTTGAATTGGTGTATATCATGAAGCCTTGTGAACTAAGTTTTGTGTATATATTAAAAAAA
 AATCAGTGTTTAAATAAAGACCTATGACTTAATCCTTTAACTCTGCGGATAGCATTGGTAGGTAGTATTAAGTGTGAATAATAAATACACA
 ATGAATTTCAATGGAAGCCATCGCCAAATATGACTTCAAAGCTACTGCAGACGACGAGCTGAGCTTCAAAGGGGGGACATCCTCAAG
 GTTTTGAACGAAGAATGTGATCAGAAGTGTACAAGGCAGAGCTTAATGGAAAAGACGGCTTCAATCCCAAGAACTACATAGAAATGAAA
 CCACATCCGTGGTTTTTTGGCAAATCCCCAGAGCCAAG

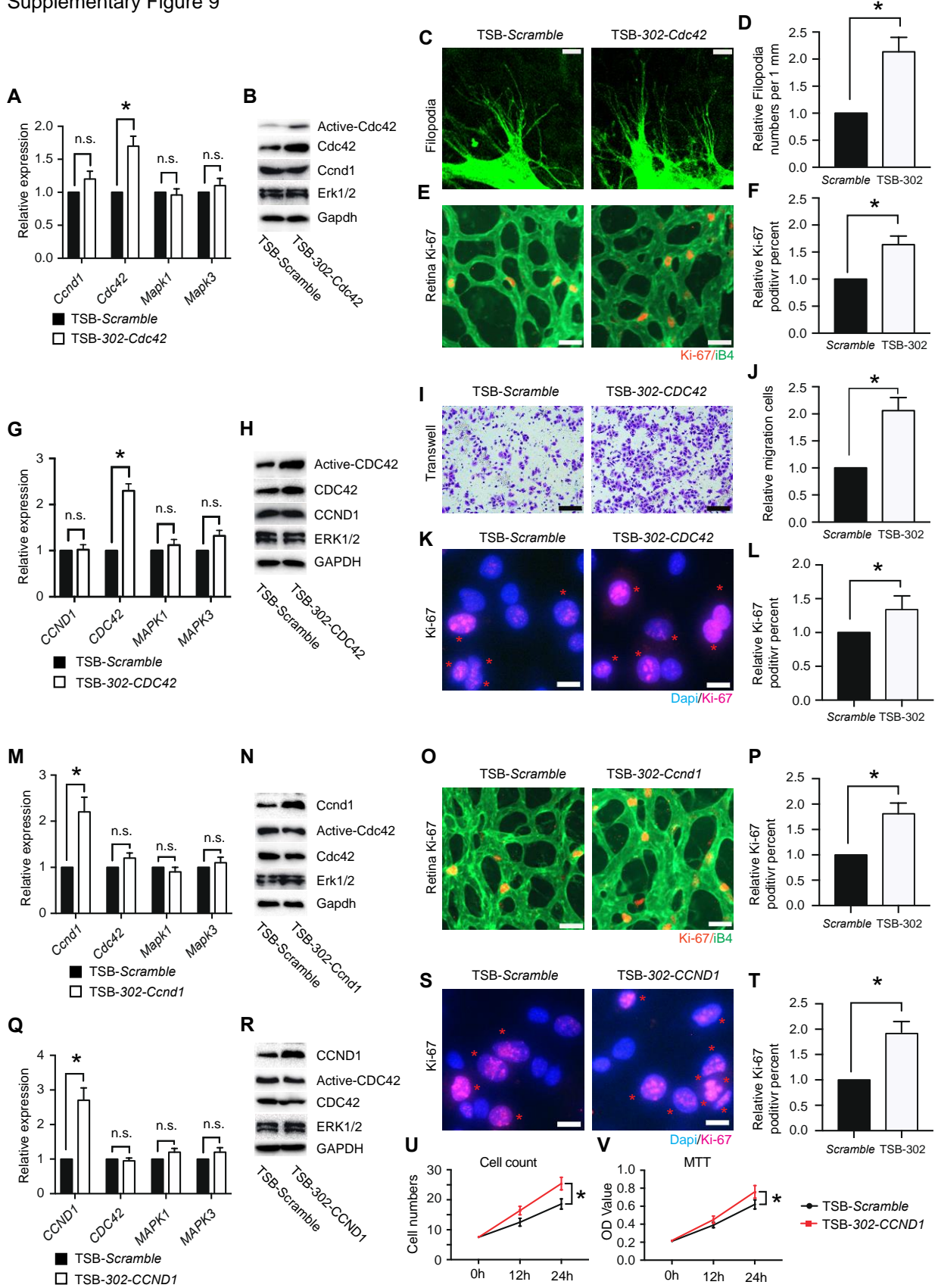
C



Supplementary Figure 7. GRB2 promoter sequence analysis. (A) *GRB2* promoter sequence has four KLF2 binding sites. (B) Sequencing result shows that -820 - +207 segment of *GRB2* promoter was successfully cloned into the pGL3 basic vector. (C) PubMed blast result shows that the cloned -820 - +207 segment located in the site of *GRB2* promoter.

Supplementary Figure 8. The sequence of mouse and human immature stem-loop and mature miR302a-d and validation of the mechanisms of Target Site Blockers for the pathways miR302 effects on. (A-D) Mouse and human sequence of immature stem-loop (A, C) and mature miR302a-d (B, D). (E) Target Site Blocker (TSB) blocks miR302 specific target gene CCND1/Ccnd1 among multiple target genes to determine the pathway responsible for cell proliferation. (F) Target Site Blocker (TSB) blocks miR302 specific target gene CDC42/Cdc42 among multiple target genes to determine the pathway responsible for cell migration. (G) The predicted consequential pairing of miR-302 with the Cdc42/Ccnd1 target region. (H) The custom-design TSB sequences to selective impair miR302 cluster-mediated inhibition of Cdc42/CDC42 or Ccnd1/CCND1.

Supplementary Figure 9



Supplementary Figure 9. Target Site Blockers confirm the important role of miR302-Cdc42/Ccnd1 pathway in EC migration and proliferation. (A-B) Mouse TSB-miR302-Cdc42 blocks the binding of miR302 to Cdc42 and enhances Cdc42 expression in ECs compared to the scrambled sequence in RNA (A) and protein (B) level without significant influence on Ccnd1 and Mapk1/3. (C-D) Mouse TSB-miR302-Cdc42 results in significant reversal of the mir302-mediated reduced angiogenic sprouting filopodia, the representative image (C) and quantification (D). (E-F) Mouse TSB-miR302-Cdc42 results in significant reversal of the mir302-mediated reduced EC proliferation shown by Ki67/IB4 co-immunostaining, the representative image (E) and quantification (F). (G-H) Human TSB-miR302-CDC42 blocks the binding of miR302 to CDC42 and enhances CDC42 expression in ECs compared to the scrambled sequence in RNA (G) and protein (H) level without significant influence on CCND1 and MAPK1/3. (I-L) Human TSB-miR302-CDC42 reversed the miR302-mediated reduced EC migration (I-J) and proliferation (K-L). (M-N) Mouse TSB-miR302-Ccnd1 blocks the binding of miR302 to Ccnd1 and enhances Ccnd1 expression in ECs compared to the scrambled sequence in RNA (M) and protein (N) level without significant influence on Cdc42 and Mapk1/3. (O-P) Mouse TSB-miR302-Ccnd1 results in significant reversal of the miR302-mediated reduced Ki67 immunostaining in *in vivo* developmental angiogenesis. (Q-R) Human TSB-miR302-CCND1 blocks the binding of miR302 to CCND1 and enhances CCND1 expression in ECs compared to the scrambled sequence in RNA (Q) and protein (R) level without significant influence on CDC42, and MAPK1/3. (S-V) Human TSB-miR302-CDC42 reversed the miR302-mediated reduced EC proliferation as shown by Ki67 staining (S-T) and cell count (U) and MTT assay of HUVECs (V). Data quantification is mean \pm S.E.M. (n = 3). All data were analyzed using Student's t-test unless otherwise noted. *, P<0.05. Scale bars: C, 50 μ m; E, 50 μ m; I, 100 μ m; K, 25 μ m; O, 50 μ m; S, 25 μ m.

Supplementary video 1: Dynamic cell motility change of HUVECs when elevated miR302-367 expression comparing to the lentiviral-GFP control.